DALTON
FULL PAPER

Crystal structure, redox and spectral properties of copper(II) complexes with macrocyclic ligands incorporating both oxamido and imine groups

En-Qing Gao,[a] Wei-Ming Bu,[b] Guang-Ming Yang,[a] Dai-Zheng Liao,*[a] Zong-Hui Jiang,[a] Shi-Ping Yan[a] and Geng-Lin Wang[a]

[a] *Department of Chemistry, Nankai University, Tianjin, 300071, P. R. China. E-mail: coord@sun.Nankai.edu.cn*
[b] *Laboratory of Supramolecular chemistry and spectroscopy, Jilin University, Changchun 130023, P. R. China*

Received 17th January 2000, Accepted 13th March 2000
Published on the Web 31st March 2000

The electrochemical and spectral behaviors of three copper(II) complexes [CuL^1] **1**, [CuL^2] **2** and [CuL^3] **3**, where L^1, L^2 and L^3 are the dianions of macrocyclic oxamido Schiff bases, have been investigated by cyclic voltammetry, electronic and ESR spectra. These macrocyclic complexes, which incorporate both oxamido and imine groups, can undergo quasi-reversible reduction ($Cu^{II} \longrightarrow Cu^{I}$) and oxidation ($Cu^{II} \longrightarrow Cu^{III}$). The crystal structures of **1** and **2** have been determined by single-crystal X-ray analysis. The difference in ring size leads to significant differences in molecular and crystal structure, electronic and ESR spectra and redox behavior. In the [14]N_4 macrocyclic complex, **2**, the CuN_4 chromophore assumes a nearly square-planar co-ordination geometry, but the geometry in the [15]N_4 macrocyclic complex, **1**, is distorted towards tetrahedral. The results from spectroscopic and redox studies are consistent with the crystallographic results and perfectly related to each other. The main factors that determine the relative stability of Cu^{I} and Cu^{III} in these complexes are the size, geometry and flexibility of the co-ordination cavity.

Introduction

Redox-active transition metal complexes that stabilize various oxidation states of the metal centers are of considerable interest, because of their potential significance as models of redox metalloenzymes[1,2] and as effective redox reactants or catalysts.[3,4] Furthermore, a recently emerged field of research concerns the use of redox-active metal complexes, for instance, copper(II) complexes with salen and related Schiff bases, as synthetic chemical nucleases or DNA damaging agents.[5] For a specific metal ion, the main factors that determine the redox properties include the nature and the arrangement of the donor atoms around the metal, which determine the ligand field, and other structural characteristics of the ligands such as the flexibility of the metal bonding site and the nature and the position of substituents. Among various ligands, many Schiff bases derived from salicylaldehyde and related aromatic aldehydes have been found to stabilize copper(I), with the Cu(II/I) potential varying from −1.4 to −0.3 V,[6] while many polyaza ligands containing deprotonated amide groups, which are strong σ donors, tend to stabilize the copper(III) state, as has been found in copper(II) complexes of oligopeptides,[5,7] oxamides[8,9a] and oxamates.[9] In addition, many copper(II) complexes of tetraazamacrocyclic ligands, which are also of great biological importance, have been electrochemically investigated.[10–13] Polyoxotetraazamacrocyclic ligands, which contain deprotonated amide groups, can also stabilize copper(III), the Cu(II/III) potential depending upon, among other factors, the ring size.[11,13] From these points of view, macrocyclic ligands bearing the dual features of amides and Schiff bases are of great interest. In fact, only a limited number of copper(II) complexes of macrocyclic ligands incorporating oxamido and imine groups have been synthesized.[14,15] Since these mononuclear complexes contain unbridged oxamido groups, they can be used as precursors for heteropolynuclear complexes, as has been done by us very recently.[15] However, to our knowledge, no copper(II) complex of this type has been crystallographically and electrochemically characterized.

With the above points in mind, we report here the redox and spectroscopic properties of three copper(II) complexes with [15]N_4 and [14]N_4 macrocyclic oxamido Schiff bases **1**–**3**, as shown. The crystal and molecular structures of **1** and **2** are also reported. The structural information allows us to justify the differences in the redox and spectral behaviors of the complexes, mainly in terms of the match between the metal cation and the dimensions or the geometry of each macrocyclic co-ordination cavity.

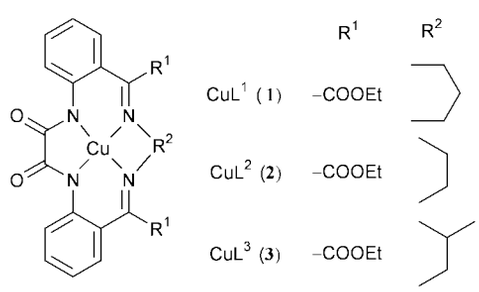

Experimental

Materials and syntheses

All chemicals were of A.R. grade and used as received, except those for electrochemical measurements. The salt *n*-Bu_4NClO_4 was recrystallized from pentane–ethyl acetate and dried under vacuum. Acetonitrile was purified by distillation from calcium hydride under a N_2 atmosphere.

The polycrystalline samples of [CuL^1] **1**, [CuL^2] **2** and [CuL^3] **3** were prepared by the template reactions of 2,2′-(oxalyldi-

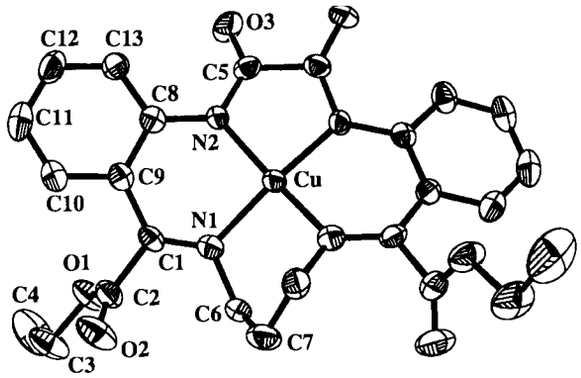

Fig. 1 An ORTEP[17] drawing of complex **1** with the atom numbering scheme.

imino)bis(phenyl glyoxylate) with appropriate diamines and copper(II) acetate in the presence of triethylamine as described elsewhere.[15a] Slow evaporation of ethanol solutions of **1** and **2** yielded red single crystals suitable for X-ray analyses.

Physical measurements

UV-Visible spectra in acetonitrile were recorded on a Shimadzu UV-2101PC UV-VIS scanning spectrophotometer, and X-band ESR spectra on a Bruker ER 200 D-SRC ESR spectrometer.

Cyclic voltammetry was performed with a BAS-100B electrochemical analyzer in 0.1 mol dm^{-3} acetonitrile solutions of *n*-Bu_4NClO_4 at room temperature. A three-electrode cell was employed with a platinum working electrode, a platinum wire auxiliary electrode and a saturated calomel reference electrode. The solutions were deaerated by an argon stream prior to all measurements, and were kept under argon during the measurements. All formal potentials were taken as the average of the anodic and cathodic peak potentials ($E_{1/2}$) and are referred to the saturated calomel electrode (SCE). Ferrocene was added after each run as an internal standard, and the ferrocenium–ferrocene couple was observed at 0.400 V at a scan rate of 100 mV s^{-1}.

Crystallography

Intensity data for single crystals of complex **1** and **2** were collected on a Siemens P4 diffractometer. The structures were solved by direct methods and subsequent Fourier difference techniques, and refined anisotropically by full-matrix least squares on F^2.[16] Crystal data and structure refinements are summarized in Table 1.

CCDC reference number 186/1896.

See http://www.rsc.org/suppdata/dt/b0/b000504p/ for crystallographic files in .cif format.

Results and discussion

Description of the structures

[CuL^1] 1. The structure of complex **1** consists of the neutral copper(II) complex of the [15]N_4 macrocyclic oxamido dianion. A perspective view of **1** with the atom numbering scheme is depicted in Fig. 1 and selected bond lengths and angles are listed in Table 2. The copper atom lies on a twofold axis that passes through the C7 atom and the center of the C–C bond of the oxamido group, and consequently the molecule has a C_2 symmetry. The macrocyclic ligand co-ordinates to the copper atom *via* two deprotonated oxamido nitrogens and two imine nitrogens. The copper atom resides right in the mean plane of the four donor atoms, and the deviations from the mean plane are ±0.240 Å for N1 and N1^I and ±0.254 Å for N2 and N2^I. Consequently, the CuN_4 chromophore assumes a square-planar geometry with an appreciable distortion towards tetrahedral. The C1–N1 (imine) distance (1.290 Å) is typical of C=N bonds.

Table 1 Summary of crystal data for [CuL^1] **1** and [CuL^2] **2**

	1	**2**
Formula	$C_{25}H_{24}CuN_4O_6$	$C_{24}H_{22}CuN_4O_6$
Formula weight	540.02	526.00
Crystal system	Monoclinic	Monoclinic
Space group	*C*2/*c*	*C*2/*c*
a/Å	24.859(3)	23.871(3)
b/Å	13.2164(10)	8.0074(12)
c/Å	7.0968(6)	25.775(3)
β/°	96.19(2)	115.663(8)
U/Å^3	2318.0(4)	4440.8(10)
Z	4	8
μ(Mo-Kα)/cm^{-1}	9.93	10.30
T/K	293(2)	293(2)
Reflections measured	2411	3906
Unique reflections	2048	3094
R(int)	0.0428	0.0452
*R*1, *wR*2 [$I > 2\sigma(I)$]	0.0578, 0.1331	0.0492, 0.0817
*R*1, *wR*2 (all data)	0.0626, 0.1537	0.0618, 0.1062

Table 2 Selected bond lengths (Å) and angles (°) with e.s.d.s in parentheses[a]

Complex **1**			
Cu–N(2)	1.923(4)	N(1)–C(1)	1.290(6)
Cu–N(1)	1.965(4)	N(1)–C(6)	1.474(6)
Cu · · · O(3^{II})	2.986(4)	N(2)–C(5)	1.355(6)
Cu · · · Cu^{III}	5.0339(13)	N(2)–C(8)	1.397(6)
N(2)–Cu–N(2^I)	87.4(2)	C(1)–N(1)–C(6)	121.1(4)
N(2)–Cu–N(1^I)	165.3(2)	C(1)–N(1)–Cu	126.1(4)
N(2)–Cu–N(1)	92.7(2)	C(6)–N(1)–Cu	112.6(3)
N(1^I)–Cu–N(1)	90.9(2)	C(5)–N(2)–C(8)	121.3(4)
N(2)–Cu–O(3^{II})	89.6(2)	C(5)–N(2)–Cu	112.2(3)
N(1)–Cu–O(3^{II})	101.12(14)	C(8)–N(2)–Cu	126.4(3)
N(2)–Cu–O(3^{III})	93.60(14)	N(1)–C(1)–C(9)	124.0(5)
N(1)–Cu–O(3^{III})	75.7(2)	N(1)–C(1)–C(2)	119.7(5)
O(3^{II})–Cu–O(3^{III})	175.54(14)	C(9)–C(1)–C(2)	116.3(4)
Complex **2**			
Cu–N(1)	1.915(5)	N(1)–C(7)	1.396(8)
Cu–N(3)	1.919(5)	N(2)–C(5)	1.275(7)
Cu–N(2)	1.943(5)	N(2)–C(3)	1.479(8)
Cu–N(4)	1.951(5)	N(3)–C(2)	1.353(8)
Cu · · · O(5^I)	3.095(6)	N(3)–C(13)	1.392(8)
Cu · · · Cu^I	6.220(2)	N(4)–C(6)	1.288(8)
N(1)–C(1)	1.360(8)	N(4)–C(4)	1.466(8)
N(1)–Cu–N(3)	87.0(2)	C(1)–N(1)–Cu	108.6(4)
N(1)–Cu–N(2)	93.9(2)	C(7)–N(1)–Cu	127.1(5)
N(3)–Cu–N(2)	177.8(3)	C(5)–N(2)–C(3)	121.2(6)
N(1)–Cu–N(4)	172.1(3)	C(5)–N(2)–Cu	126.7(5)
N(3)–Cu–N(4)	93.5(2)	C(3)–N(2)–Cu	111.9(4)
N(2)–Cu–N(4)	85.9(2)	C(2)–N(3)–C(13)	123.0(6)
N(1)–Cu–O(5^I)	75.2(2)	C(2)–N(3)–Cu	111.5(5)
N(3)–Cu–O(5^I)	86.2(2)	C(13)–N(3)–Cu	125.4(5)
N(2)–Cu–O(5^I)	96.0(2)	C(6)–N(4)–C(4)	123.8(6)
N(4)–Cu–O(5^I)	97.0(2)	C(6)–N(4)–Cu	125.3(5)
C(1)–N(1)–C(7)	122.7(6)	C(4)–N(4)–Cu	110.7(4)

[a] Symmetry codes: complex **1**, I $-x,y,-z+\frac{3}{2}$; II $x,-y+1,z-\frac{1}{2}$; III $-x,y+1,-z+2$; **2**, I $-x+2,-y+2,-z+1$.

The Cu–N2 (amido) bond (1.923 Å) is shorter than the Cu–N1 (imine) bond (1.965 Å), consistent with the stronger donor ability of the deprotonated amido nitrogen compared to the imine nitrogen. The two symmetry-related phenyl rings tilt on the opposite side of the N_4 plane with a dihedral angle of 26.4°. The six-membered diimine chelate ring assumes a twist conformation.[18]

In the crystal of complex **1** the neutral molecules are stacked in such an offset way that the two "vacant" co-ordination sites above and below the CuN_4 moiety are occupied by the oxamido oxygens (O3^{II} and O3^{III}) arising from two adjacent molecules, with an interatomic Cu · · · O distance of 2.986 Å, indicative of

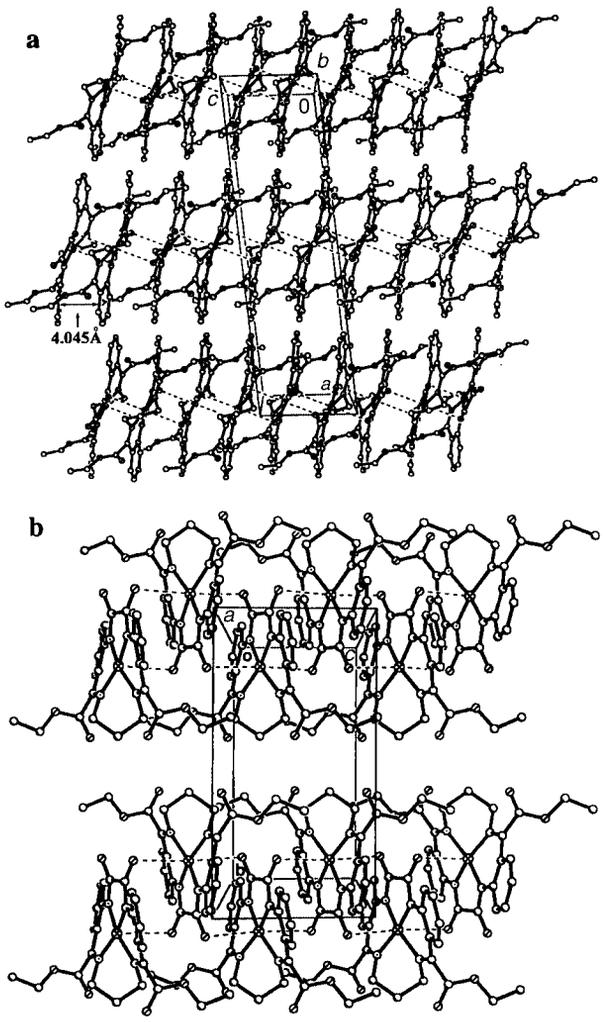

Fig. 2 Projections of the quasi-1-D chain formed along the *c* axis *via* intermolecular interactions in the crystal structure of complex **1**: (a) down the *b* axis and (b) down the *a* axis.

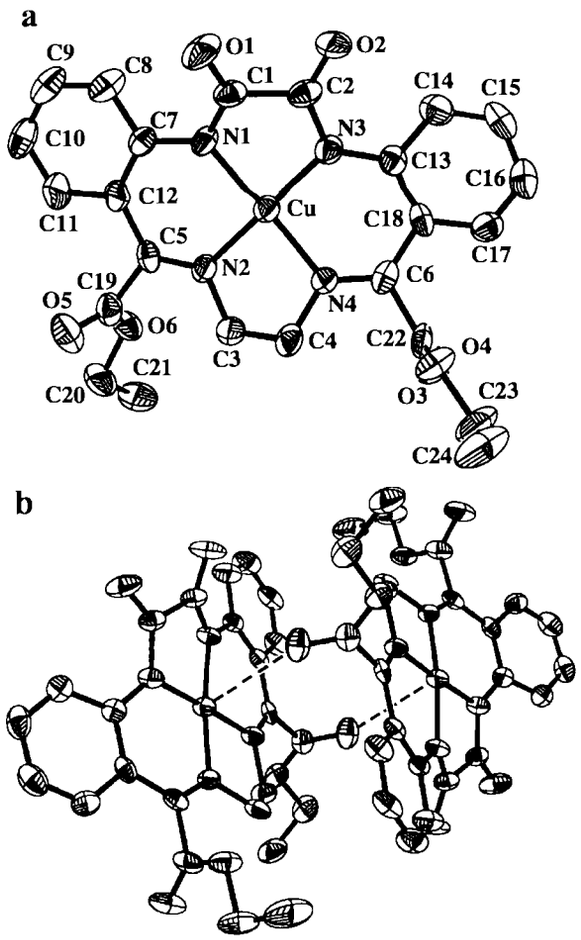

Fig. 3 ORTEP drawings of complex **2**: (a) the molecular structure with the atom numbering scheme and (b) the quasi-dimer structure formed *via* weak co-ordination bonds.

weak co-ordination bonds. Taking into account the weak interactions, the copper atom may be said to be in a highly elongated octahedral N_4O_2 environment. In addition, each two neighboring phenyl rings related by the $(x, -y + 1, z - \frac{1}{2})$ transformation are inclined towards each other at a dihedral angle of 17.9° and separated by 4.045 Å, indicating the presence of weak π–π stacking interactions (Fig. 2a). As a result of the above two types of weak intermolecular interactions, the [CuL^1] molecules are stacked along the *c* axis to form a quasi-one-dimensional chain, in which copper atoms are arranged in a zigzag fashion (Fig. 2b). The nearest intrachain Cu · · · Cu distance is 5.034 Å.

[CuL^2] 2. The structure of complex **2** consists of the neutral copper(II) complex of the [14]N_4 macrocyclic oxamido anion. A perspective view of **2** with the atom numbering scheme is depicted in Fig. 3 and selected bond lengths and angles are listed in Table 2. The copper atom in **2** is 0.048 Å out of the mean plane of the four nitrogen donors from the macrocyclic ligand, and the deviations of all the nitrogen atoms from the plane are ±0.084 Å, much less than those in **1.** Consequently, the metal ion is in a slightly distorted square-planar environment, which is obviously different from that in **1**. The N_4 plane is approximately coplanar with the two phenyl rings, which tilt slightly on the same side of the N_4 plane, and the dihedral angles of the N_4 plane with the C7–C8–C9–C10–C11–C12 and C13–C14–C15–C16–C17–C18 planes are 9.5 and 17.5°, respectively. These dihedral angles are smaller than that observed in **1**, suggesting that somewhat more efficient π delocalization is present in the [14]N_4 macrocyclic molecule. The five-membered diimine chelate ring assumes a *gauche* conformation[18] and the diimine chelate angle (N2–Cu–N4, 85.9°) is smaller than that in **1** (N1–Cu–$N1^I$, 90.9°), the other three chelate angles being practically identical to those in **1**. Furthermore, the Cu–N distances for both imino and amido nitrogens are shorter than those in **1**, suggesting stronger co-ordination bonding in **2**. These structural features indicate that the co-ordination cavity in the [14]N_4 macrocyclic complex is smaller than that in the [15]N_4 species.

The closest contact between adjacent molecules is Cu · · · O5$(2 - x, 2 - y, 1 - z)$ (3.095 Å), indicating the presence of a weak co-ordination bond. As a result of the weak intermolecular interaction, a quasi-dimer is formed between two [CuL^1] complexes related by an inversion center (Fig. 3), with a Cu · · · Cu distance of 6.220 Å. Therefore, one may say that the co-ordination geometry of the copper atom in **2** is a quasi-square pyramid. No intra- or inter-dimer π–π stacking interactions between phenyl rings are evident.

The differences in intermolecular interactions and consequently in the crystal structures of **1** and **2** are most likely due to the difference in the cavity sizes of the two macrocycles. The [15]N_4 macrocycle (L^1), which is derived from 1,3-diaminopropane and contains a six-membered diimine chelate rings, has a larger co-ordination cavity than the [14]N_4 macrocycle (L^2), which contains a five-membered diimine chelate ring imposed by the ethylenediimine group. Therefore, the metal atom in **1** is located right in the cavity, leaving a "vacant" site for weak co-ordination bonding on each side of the CuN_4 moiety, while the metal ion in **2** is slightly displaced out of the cavity and prefers to form one weak co-ordination bond on only one side, towards which Cu is displaced, and the co-ordination on the other side is precluded by steric effects.

Table 3 Summary of physical data for complexes **1**, **2** and **3**

Complex	ESR[a]						Cu(II/I)[b]		Cu(II/III)[b]	
	$g_{\|}$	$g_{\perp}$[c]	g_{iso}[d]	A_{iso}[d]	$A_{\|}$[e]	λ_{max}/nm (ε/M^{-1} cm^{-1})	$E_{1/2}$/V	ΔE_p/mV	$E_{1/2}$/V	ΔE_p/mV
1	2.169[c] 2.175[e]	2.038	2.084	81.3	164	286 (22600), 374 (13400), 415 (8400), 636 (150)	−1.015	102	1.036	98
2	2.145[c] 2.156[e]	2.035	2.078	88.7	183	287 (21500), 376 (12700), 420 (7600), 542 (185)	−1.130	117	0.976	92
3	2.146[c] 2.155[e]	2.031	2.077	88.8	187	287 (21100), 372 (11500), 420 (8100), 540 (200)	−1.125	92	0.986	85

[a] A values are in 10^{-4} cm^{-1}. [b] Scan rate = 100 mV s^{-1}. $E_{1/2}$ values (*vs.* SCE) were taken as the averages of the anodic peak potentials (E_{pa}) and the cathodic (E_{pc}) peak potentials, $\Delta E_p = |E_{pa} - E_{pc}|$. [c] Values calculated from polycrystalline spectra. [d] Values calculated from solution spectra in acetonitrile at room temperature. [e] Values estimated from frozen solution spectra in acetonitrile at 77 K.

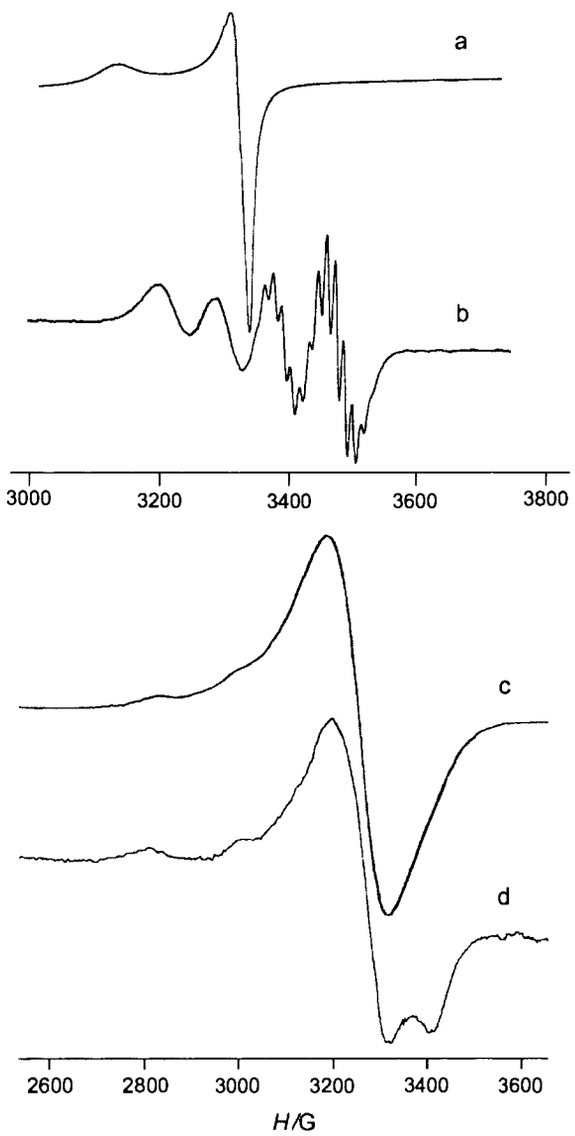

Fig. 4 X-Band ESR spectra of (a) a polycrystalline sample of complex **1** (9.486 GHz), (b) an acetonitrile solution of **1** at room temperature (9.775 GHz), (c) an acetonitrile solution of **1** at 77 K (9.425 GHz), (d) an acetonitrile solution of **2** at 77 K (9.430 GHz).

Spectroscopic studies

The X-band room-temperature ESR spectra of polycrystalline samples and acetonitrile solutions of complex **1**, together with the frozen solution spectra of **1** and **2** in acetonitrile at 77 K, are shown in Fig. 4. The room-temperature spectra of **2** and **3** are similar to those of **1**, and the frozen solution spectrum of **3** is similar to that of **2**. The parameters obtained from the spectra are listed in Table 3. The solid spectra are axial

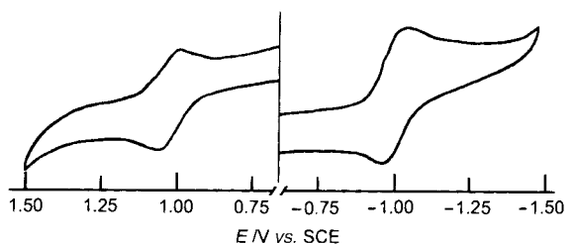

Fig. 5 Cyclic voltammogram for complex **1** in acetonitrile at 100 mV s^{-1}.

with $g_{\|} > g_{\perp} > 2.02$, typical of a copper(II) (d^9) ion in axial symmetry with the unpaired electron present in the $d_{x^2-y^2}$ orbital.[19,20] The room-temperature solution spectra show hyperfine splitting lines characteristic of copper(II) complexes, and superhyperfine splitting lines due to the co-ordinated nitrogen atoms (a_N = 13 G). The hyperfine splittings were also observed in frozen solutions. The $g_{\|}$, $A_{\|}$ and A_{iso} values for four-co-ordinate copper(II) complexes with similar ligands carry information about the co-ordination geometry around the metal ion.[20–22] It has been revealed experimentally and theoretically that, on going from a square-planar geometry to a corresponding tetrahedrally distorted one, the $g_{\|}$ value increases and the $A_{\|}$ and A_{iso} values decrease. As is shown in Table 3, the two [14]N_4 complexes **2** and **3** show no significant difference in $g_{\|}$, A_{iso} and $A_{\|}$, but the $g_{\|}$ value of the [15]N_4 complex **1** is significantly larger, and its A_{iso} and $A_{\|}$ values are significantly smaller, compared with those of **2** and **3**. This fact, combined with the visible spectral results (see below), indicates that the N_4 co-ordination cavity of **1** in the solution is significantly distorted towards tetrahedral, as has been revealed by X-ray analysis in the solid state.

The electronic absorption spectra of complexes **1**, **2** and **3** in acetonitrile exhibit essentially similar patterns in the 250–500 nm region, with three strong bands due to intraligand and charge-transfer transitions. A broad and much less intense band for **1** was observed at 636 nm, assignable to envelope of the d–d transitions of Cu^{II} in an environment close to square planar.[9,20] The corresponding d–d bands for **2** and **3** appear at 542 and 540 nm, respectively, as shoulders of the near-ultraviolet bands. The significant red shift in the maximum of the d–d band for **1** relative to those for **2** and **3**, in spite of the presence of the same CuN_4 chromophore, indicates that a weaker ligand field is associated with the [15]N_4 macrocyclic ligands compared with the [14]N_4 ones.[9] This is consistent with the larger $g_{\|}$ value, the tetrahedral distortion of the co-ordination geometry[20,22] and the longer Cu–N distances in **1**, as demonstrated by crystallographic studies.

Redox studies

The three complexes exhibit similar electrochemical behavior. The cyclic voltammograms in acetonitrile are exemplified by that of **1** in Fig. 5 and the data collected in Table 3. All the

complexes show two quasi-reversible redox processes in the 1.5–−1.5 V *vs.* SCE potential range. The wave detected at negative potentials ($E_{1/2}$ = −1.02 to −1.13 V *vs.* SCE) is assignable to the Cu(II/I) couple and the other at positive potentials ($E_{1/2}$ = 0.976 to 1.036 V *vs.* SCE) to the Cu(II/III) couple. The suggestion that the redox processes are metal centered is based on the following considerations. First, although the "free" macrocyclic ligand is not available, its precursor, diethyl 2,2′-(oxalyldiimino)-bis(phenyl glyoxylate), and related Schiff bases derived from salicyldaldehydes, show no redox wave in the experimental potential range. Secondly, if the processes were ligand centered, different aliphatic diimine fragments would not cause significant differences in formal potentials. In fact, although the two $[14]N_4$ complexes **2** and **3** undergo redox processes at nearly the same potential, the $[15]N_4$ complex **1** shows significant shifts in the formal potentials of both couples: the Cu(II/I) potential is less negative and the Cu(II/III) one is more positive.

The difference in the formal potentials can be rationalized in terms of the flexibility and the size of the co-ordination cavity in the complexes, and the geometric requirements and the size of the metal ions in different oxidation states. The reduction of Cu^{II} (d^9) to Cu^{I} (d^{10}) involves a drastic increase in the metal radius and a configuration change from square planar to tetrahedral. Obviously, the larger and more flexible 15-membered co-ordination cavity with a tetrahedral distortion in **1**, compared with the 14-membered one in **2** and **3**, tends to stabilize the copper(I) complex, so the Cu(II/I) formal potential for **1** is less negative than those for **2** and **3**. On the other hand, Cu^{III} (d^8) tends to assume a square-planar co-ordination geometry with a low-spin ground state, and the oxidation of Cu^{II} to Cu^{III} involves a drastic reduction in ionic radius. In comparison with the tetrahedrally distorted 15-membered co-ordination cavity in **1**, the smaller and more nearly coplanar 14-membered cavity in **2** and **3** seems to fit Cu^{III} better, thus tending to stabilize the copper(III) complexes, so the Cu(II/III) potentials for **2** and **3** are less positive than that for **1**.

The spectral and redox data listed in Table 3 reveal that complex **1**, which exhibits a significantly red-shifted d–d absorption, relatively increased $g_{\|}$ and decreased A_{iso} values, has a less negative Cu(II/I) potential and a more positive Cu(II/III) potential than those of **2** and **3**, indicating that there may be correlations between the spectral and redox properties of these complexes. These phenomena have also been found for some other copper(II) complexes. Red shifts in d–d absorption maxima for a series of macrocyclic copper(II) complexes[10d] and a number of copper(II) complexes with N-substituted hydroxynaphthaldimines[6a] have been related to stabilization of Cu^{I}. On the other hand, blue shifts in d–d maxima observed for a large number of peptide–copper(II) complexes[7] and a recently reported class of substituted oxamido- and oxamato-copper(II) complexes[9] are related to stabilization of Cu^{III}. A linear relation has also been established between $g_{\|}$ and the Cu(II/I) potential for a series of macrocyclic copper(II) complexes.[10d] These relationships reflect the relative loss in crystal-field stabilization energy (CFSE) on reduction from d^9 to d^{10} and the relative gain in CFSE on oxidation from d^9 to d^8 (low-spin). As discussed above, all the spectral data for **1**, the lower-frequency d–d absorption and the larger $g_{\|}$ and smaller A_{iso} values, are indicative of a weaker ligand field. A weaker ligand field around Cu^{II} leads to a smaller loss in CFSE on reduction and a smaller gain in CFSE on oxidation, thus relatively stabilizing Cu^{I} and destabilizing Cu^{III}.

In conclusion, the results from crystallographic, spectroscopic and redox studies on the present complexes are consistent with and related to one another very well. This contribution reveals that the present copper(II) complexes can undergo both quasi-reversible reduction ($Cu^{II} \longrightarrow Cu^{I}$) and oxidation ($Cu^{II} \longrightarrow Cu^{III}$), and thus demonstrates that the macrocyclic ligands incorporating both oxamido and imine groups can stabilize both Cu^{I} and Cu^{III}. The main factors that determine the relative stability of Cu^{I} and Cu^{III} in these complexes are the size, geometry and flexibility of the co-ordination cavity. It seems to us worthwhile to extend this work by synthesizing more macrocyclic systems with different ring sizes and by introducing substituents into the macrocycles, to get a more complete picture of the factors that influence the redox behavior. It would contribute to the synthesis of model compounds and help our understanding of the functioning of metalloproteins related to electron transport. Further work along this line is in progress.

Acknowledgements

This work was supported by the Natural Science Foundation of China (Nos. 59772020 and 29631040) and Natural Science Foundation of Tianjin (No. 983604611).

References

1 R. H. Holm, P. Kennepohl and E. I. Solomon, *Chem. Rev.*, 1996, **96**, 2239; J. P. Klinman, *Chem. Rev.*, 1996, **96**, 2541; S. Ferguson-Miller and G. T. Babcock, *Chem. Rev.*, 1996, **96**, 2889; N. Kitajima and Y. Moro-oka, *Chem. Rev.*, 1994, **94**, 737.

2 N. Ito, S. E. V. Philips, C. Stevenns, Z. B. Ogel, M. J. McPherson, G. N. Keen, K. D. S. Yadav and P. F. Knoeles, *Nature* (*London*), 1991, **350**, 87; M. Vaidyanathan, R. Viswanathan, M. Palaniandavar, T. Balasubramanian, P. Prabhaharan and T. P. Muthiah, *Inorg. Chem.*, 1998, **37**, 6418.

3 T. R. Wagler and C. J. Burrows, *Tetrahedron Lett.*, 1988, **29**, 5091; T. R. Wagler, Y. Fang and C. J. Burrows, *J. Org. Chem.*, 1989, **54**, 1564; W. Adam, R. T. Fell, V. R. Stegmann and C. R. Saha-Möller, *J. Am. Chem. Soc.*, 1998, **120**, 708.

4 K. Nag and A. Chakravorty, *Coord. Chem. Rev.*, 1980, **33**, 87; D. W. Margerum and G. D. Owens, in *Metal Ions in Biological Systems*, ed. H. Sigel, Marcel Dekker Inc., New York, 1981, vol. 12, p. 75; T. F. Collins, *Acc. Chem. Res.*, 1994, **27**, 279.

5 E. Lammour, S. Routier, J.-L. Bernier, J.-P. Catteau, C. Bailly and H. Vezin, *J. Am. Chem. Soc.*, 1999, **121**, 1862 and refs. therein; C. J. Burrows and J. G. Muller, *Chem. Rev.*, 1998, **98**, 1109.

6 (*a*) J. Costamagana, J. Vargas, R. Latorre, A. Alvarado and G. Mena, *Coord. Chem., Rev.*, 1992, **119**, 67 and refs. therein; (*b*) B. E. Bursten and M. R. Green, *Prog. Inorg. Chem.*, 1988, **36**, 474.

7 M. R. McDonald, W. M. Scheper, H. D. Lee and D. W. Margerum, *Inorg. Chem.*, 1995, **34**, 229; F. P. Bossu, K. L. Chellappa and D. W. Margerum, *J. Am. Chem. Soc.*, 1977, **99**, 2195; A. G. Lappin, C. K. Murry and D. W. Margerum, *Inorg. Chem.*, 1978, **17**, 1630; L. L. Diaddario, W. R. Robinson and D. W. Margerum, *Inorg. Chem.*, 1983, **22**, 1021.

8 J. J. Bour and J. J. Steggerda, *Chem. Commun.*, 1967, 85; J. J. Bour, P. J. M. W. L. Birker and J. J. Steggerda, *Inorg. Chem.*, 1971, **10**, 1201; F. C. Anson, T. J. Collins, T. G. Richmond, B. D. Santarsiero, J. E. Toth and B. G. R. T. Treco, *J. Am. Chem. Soc.*, 1987, **109**, 2974.

9 (*a*) R. Ruiz, C. Surville-Barland, A. Aukauloo, E. Anxolabehere-Mallart, Y. Journaux, J. Cano and M. C. Muñoz, *J. Chem. Soc., Dalton Trans.*, 1997, 745; (*b*) B. Cervera, J. L. Sanz, M. J. Ibáñez, G. Vila, F. Lloret, M. Julve, R. Ruiz, X. Ottenwaelder, A. Aukauloo, S. Poussereau, Y. Journaux, J. Cano and M. C. Muñoz, *J. Chem. Soc., Dalton Trans.*, 1998, 781.

10 (*a*) J. F. Endicott and B. Durham, in *Co-ordination Chemistry of Macrocyclic Compounds*, ed. G. A. Melson, Plenum, New York, 1979, p. 413; (*b*) P. Zanello, R. Seeber, A. Cinquantini, G.-A. Mazzocchin and L. Fabbrizzi, *J. Chem. Soc., Dalton Trans.*, 1982, 893; (*c*) D. C. Olson and J. Vasilevskis, *Inorg. Chem.*, 1971, **10**, 463; (*d*) K. Miyoshi, H. Tanaka, E. Kimura, S. Tsuboyama, S. Murata, H. Shimizu and K. Ishizu, *Inorg. Chim. Acta*, 1983, **78**, 23.

11 M. Kodama and E. Kimura, *J. Chem. Soc., Dalton Trans.*, 1979, 325; E. Kimura, *J. Coord. Chem.*, 1986, **15**, 1; M. Shionoya, E. Kimura and Y. Iitaka, *J. Am. Chem. Soc.*, 1990, **112**, 9237.

12 L. Fabbrizzi, A. Perotti and A. Poggi, *Inorg. Chem.*, 1983, **22**, 1411; Y. D. Lampeka and S. P. Gavrish, *J. Coord. Chem.*, 1990, **21**, 351; G. D. Santis, L. Fabbrizzi, M. Licchelli and P. Pallavicini, *Coord. Chem. Rev.*, 1992, **120**, 237; J. S. Rybka and D. W. Margerum, *Inorg. Chem.*, 1981, **20**, 1453.

13 F. Kou, S. Zhu, H. Lin, K. Ma and Y. Chen, *Polyhedron*, 1997, **16**, 741; X. H. Bu, D. L. An, Z. A. Zhu and Y. T. Chen, *Polyhedron*, 1997, **16**, 179.

14 D. St. C. Black, C. H. B Vanderzalm and A. J. Hartshom, *Inorg. Nucl. Chem. Lett.*, 1976, **12**, 657; D. St. C. Black, C. H. B.

Vanderzalm and C. H. Wong, *Aust. J. Chem.*, 1982, **35**, 2435; D. St. C. Black and G. I. Moss, *Aust. J. Chem.*, 1987, **40**, 129, 143.
15 (*a*) E.-Q. Gao, G.-M. Yang, D.-Z. Liao, Z.-H. Jiang, S.-P. Yan, G.-L. Wang and H.-Z. Kou, *Transition Met. Chem.*, 1999, **24**, 244; (*b*) E.-Q. Gao, G.-M. Yang, D.-Z. Liao, Z.-H. Jiang, S.-P. Yan and G.-L. Wang, *J. Chem. Res. (S)*, 1999, 278; (*c*) E.-Q. Gao, G.-M. Yang, J.-K. Tang, D.-Z. Liao, Z.-H. Jiang and S.-P. Yan, *Polyhedron*, 1999, **18**, 3643.
16 G. M. Sheldrick, SHELXS 86, Program for crystal structure solution, University of Göttingen, 1986; SHELXL 93, Program for crystal structure refinement, University of Göttingen, 1993.
17 C. K. Johnson, ORTEP II, Report ORNL-5138, Oak Ridge National Laboratory, Oak Ridge, TN, 1976.
18 N. F. Curtis, in *Co-ordination Chemistry of Macrocyclic Compounds*, ed. G. A. Melson, Plenum, New York, 1979, pp. 226 and 251; F. A. Jurnak and K. N. Raymond, *Inorg. Chem.*, 1972, **11**, 3149.
19 B. J. Hathaway and A. A. G. Tomlinson, *Coord. Chem. Rev.*, 1970, **5**, 1; B. J. Hathaway and D. E. Billing, *Coord. Chem. Rev.*, 1970, **5**, 143.
20 H. Yokoi, *Bull. Chem. Soc. Jpn.*, 1974, **47**, 3037.
21 M. Sharnoff, *J. Chem. Phys.*, 1965, **42**, 3383; B. R. McGarvey, *J. Phys. Chem.*, 1967, **71**, 51.
22 Y. Murakami, Y. Matsuda and K. Sakata, *Inorg. Chem.*, 1981, **10**, 1728, 1734.